

Electron Spectrum for the Prompt Emission of Gamma-Ray Bursts in the Synchrotron Radiation Scenario

Kuan Liu, Da-Bin Lin , Jing Li, Yu-Fei Li, Rui-Jing Lu , and En-Wei Lian GuangXi Key Laboratory for Relativistic AstrophysicSchool of Physical Science and Technolo@uangxi University.Nanning 530004People's Republic of China; lindabin@gxu.edu.cn Received 2020 September 21; revised 2021 January 26; accepted 2021 February 16; published 2021 April 9

Abstract

Growing evidence indicates that the synchrotron radiation mechanism may be responsible for the prompt emission of gamma-ray bursts (GRBs) the synchrotron radiation scenarithe electron energy spectrum of the prompt emission is diverse in theoretical works and has not been estimated from observations in a general (i.e., without specifying a certain physical model for the electron spectrum) In this paper, we creatively propose a method to directly estimate the electron spectrum for the prompt emission and specifying a certain physical model for the electron spectrum in the synchrotron radiation scenario. In this method, an empirical function (i.e., a four-order Bézier curve jointed with a linear function at high energy) is applied to describe the electron spectrum in log-log coordinates. It is found that our empirical function can well mimic the electron spectra obtained in many numerical calculations or simulations. Then, our method can figure out the electron spectrum for the prompt emission without specifying a model. By employing our method on observationstaking GRB 180720B and GRB 160509A as examples, is found that the obtained electron spectra are generally different from that in the standard fast-cooling scenario and even a broken power law. Moreover, the morphology of electron spectra in its low-energy regime varies with time in a burst and even in a pulse. Our proposed method provides a valuable way to confront the synchrotron radiation mechanism with observations.

Unified Astronomy Thesaurus concepts: Gamma-ray bursts (629); Relativistic jets (1390)

1. Introduction

The radiation mechanism for the prompt emission of gamma-ray bursts (GRBs) emains unclearafter decades of law function, i.e., Band function (Band et al. 1993). The typical magnetic field (Madret 1993) and specific field (Madret 1993). value of parametersin the Band function by fitting the observations are $\alpha \sim -1\beta \sim -2.2$, and $E_0 \sim 400$ keV, where α , β , and E_0 are the low-energy photon spectraldex, highrespectively (Preece et al. 2000; Nava et al. 2011; Kaneko et al. On the other hand it. 2006; Goldstein et al. 2012). Owing to the lack of physical origin for the Band function, one derives the physical implications by inferring what mechanism the fitparameters can be produced by. Synchrotron radiation is a very natural candidate to explain the nonthermal feature of the Band function (Meszaros et al. 1994; Tavani 1996; Daigne & Mochkovitch 1998; Ghirlanda et al. 2002). However, the most straightforward synchrotron model suffers from the "fastcooling problem," i.e., the typical observed spectrum should have a low-energy photon spectral index -3/2, which strongly conflicts with observations (Saret al. 1998; Ghisellini et al. 2000). Many attempts have been made to alleviate the fastcooling problem, e.g., adopting a decaying magnetic field in the model to fit the prompt emission with optical observations. emission region (Pe'er & Zhang 2006Uhm & Zhang 2014; Zhao et al. 2014), introducing a slow heating mechanism by magnetic turbulence (Asano & Terasawa 2009) volving the inverse Compton scattering effect at the Klein-Nishina regime efforts have been made, the functional forms adopted to (Derishev etal. 2001; Nakar et al. 2009; Florou et al. 2021), considering a marginally fast cooling regime (Daigne et al. 2011; Beniamini et al. 2018), or invoking a fast-increasing

shown that the synchrotron model could not account for about one-third of bursts with $\alpha > -2/3$, which is the so-called synchrotron "line-of-death" problem (Preece et al. 1998). There observations. The radiation spectra of the prompt emission are limit, such as considering the synchrotron self-absorption synchrotron emission from the relativistic electrons with a small pitch angle (Lloyd & Petrosian 2000; Lloyd-Ronning & Petrosian 2002; Yang & Zhang 2018), or involving the inverse

On the other hand, it has been proven that directly fitting the observations based on the synchrotron radiation model can be also effective. By adopting electron spectra composed of thermal Maxwell distribution connected to a power law at highenergy, Tavani (1996), Baring & Braby (2004), and Burgess et al. (2014) fit the observed radiation spectrum in the synchrotron radiation scenario with or without photospheric emission. Lloyd & Petrosian (2000) and Lloyd-Ronning & Petrosian (2002) investigate the synchrotron emission models as the source of GRB prompt emission spectra by involving the "smooth cutoff" to the electron spectrum. To test the radiation mechanism of the promptemission, Oganesyan etal. (2019) adopted broken power-law electron spectra in the synchrotron Zhang et al. (2016) and Burgess et al. (2020) fit the observations in the synchrotron radiation scenario by specifying a physicalmodel for the electron spectra Although many describe the electron spectra are generally model dependent. It is also worth pointing out that the electron spectrum can be very diverse in numerical calculations or simulations (e.g., Uhm electron energy injection rate (Liu et al. 2020). In addition, it is & Zhang 2014; Sironi & Spitkovsky 2009; Guo et al. 2014;

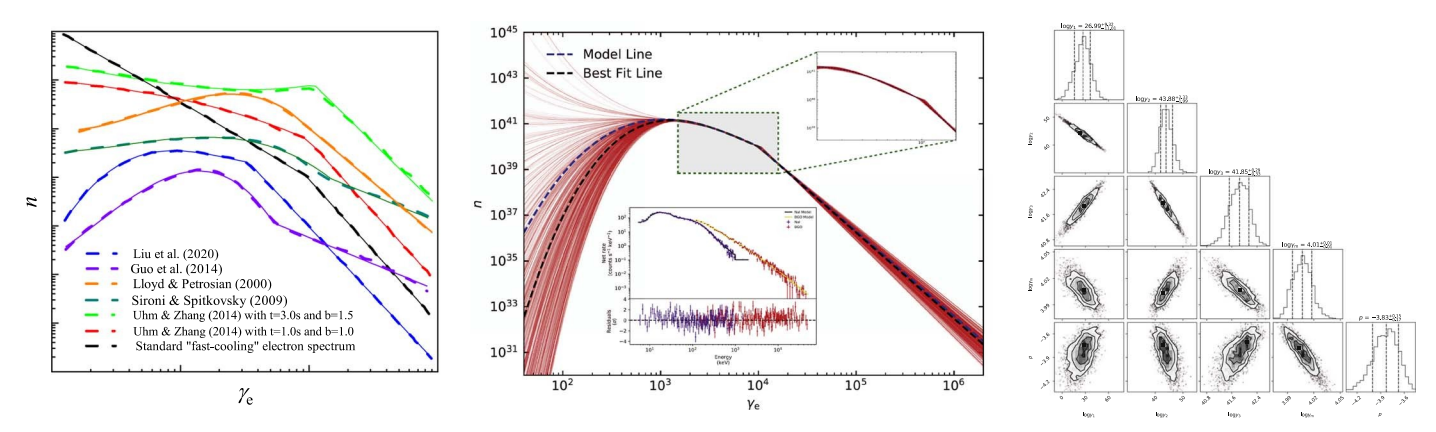


Figure 1. Testing of our empirical function (left panel) and the spectral-fitting method (middle and right panel). In the left panel, the electron spectra collected from different works and the corresponding best-fitting results with our empirical function are shown with dashed and solid lines, respectively. Here, the purple, dark gre green, red, orange, and blue dashed lines are the electron spectra obtained from Figure 1 of Guo et al. (20+47)00itlFigure 10 of Sironi & Spitkovsky (2009) with θ = 30°, the second panebf Figure 1 in Uhm & Zhang (2014) with t_{obs} = 1.0 s, the forth panel of Figure 1 in Uhm & Zhang (2014) with t_{obs} = 3.0 s, Equation (4) of Lloyd & Petrosian (2000) with q = 1.0 and p = 3.0, and Figure 1 of Liu et al. (2020) with 1.2 s, respectively. In the middle panel, the electron spectra based on the last 1% of iterations from the MCMC sampling are plotted with red limber the blue and black dashed lines represent the given electron spectrum and the best-fitting result for the electron spectrum from MCMC sampling. In addition, the upper inset shows a zoomed-in view for the electron spectrum $\gamma_e \sim 10^3 - 10^4$ and the bottom inset shows the best-fitting result on the synthetic duatance right panel, the posterior probability density functions by applying our spectral-fitting method on the synthetic data.

Liu et al. 2020). Please see Figure 1 for some examples (dash@dur-orderBézier curve to describe the low-energy electron lines). In these cases, using a model-dependentelectron spectrum in the synchrotron radiation scenario to fit the observations may bias the understanding of the prompt emission. In this paper, we propose a method to directly estimate the electron spectrum for the prompt emission, without specifying a certain physical model or presumptive morphology for the electron spectrum. This paper is organized as follows. In Section 2, we describe our proposed empirical

spectrum in log-log coordinates (i.e., $\log q$ - $\log n$ plane). Therefore, our empirical function used to describe the electron spectrum is read as

$$\log n = \begin{cases} \mathbb{I}(g_{\mathbb{P}}), & g_{\mathbb{P}} < g_{\mathbb{P}}, \\ \log[y_{\mathbb{P}}(g_{\mathbb{P}}/g_{\mathbb{P}})^{-p}], & g_{\mathbb{P}} \mathbb{I}g_{\mathbb{P}}, \end{cases}$$
(1)

where (g) is the four-order Bézier curve and the number function in detail. The empirical function is the key point of our density of electrons atγ_e = γ_m. The four-order Bézier curve method and we focus on the synchrotron radiation scenario. In $\mathbb{I}(g)$ is described with a serial of points (t), $\mathbb{I}(t)$, which are Section 3, our method is applied to discuss the Band radiation calculated with following equation by varying t from 0 to 1:

$$\begin{cases} \mathbb{I}(t) = (1 - t)^3 \log y_1 + 3t(1 - t)^2 \log y_2 + 3t^2(1 - t) \log y_3 + t^3 \log y_m, \\ \log g_{\mathbb{E}}(t) = (1 - t)^3 \log g_{\mathbb{E},1} + 3t(1 - t)^2 \log g_{\mathbb{E},2} + 3t^2(1 - t) \log g_{\mathbb{E},3} + t^3 \log g_m. \end{cases}$$
 (2)

spectrum and on spectral analysis of observations. In Section 4 Here, $P_1(\log g_{a_1}, \log y_1)$, $P_2(\log g_{a_2}, \log y_2)$, $P_3(\log g_{a_3}, \log y_3)$, we summarize our results.

2. Prescription of Electron Spectrum and Fitting Method

In this paper, we mainly focus on how to estimate the electron spectrum for the promptmission in the synchrotron radiation scenarioIn the synchrotron radiation scenariothe GRBs' prompt emission is generated from a group of relativistic electrons. Therefore, the electron energy spectrum for the prompt emission can be estimated by fitting the radiation spectrum. For this purposewe propose an empirical function to picture the possible electron spectrum.

Intuitively, the electron spectrum shown in Figure 1 can be decomposed into two segments: high-energy segmented a low-energy segmentiointed at the electron Lorentz factor $\gamma_e = \gamma_m$. The high-energy segment usually relates to the electron injection rate $Q(g_{\rm e}) \mu g_{\rm e}^{\ p}$ and can be described by a power-law function $Q(g_{\rm e}) \mu g_{\rm e}^{\ p}$, where ndy is the number of electrons in $[y_{\rm e}, y_{\rm e} + dy_{\rm e}]$. However, the morphology of the low-energy segments diverse theoretically and can be very different from a power-law function. Then, we introduce a

and $P_4(\log g_{\rm m}, \log y_{\rm m})$ are four control points used to create the Bézier curve. To simplify our fittings, we adopt $\log g_{\rm e,1} = 1$, $\log g_{\rm e,2} = (\log g_{\rm m,0} - \log g_{\rm e,1})/3 + \log g_{\rm e,1}$, and $\log g_{\rm e,3} = 2(\log g_{\rm m,0} - \log g_{\rm e,1})/3 + \log g_{\rm e,1}$, where $\gamma_{\rm m,0} = 10^4$ is set as the initial value of $\gamma_{\rm m}$. Then, the free parameters in our empirical function are y y₂, y₃, γ_m, and p. We fit the electron spectra in the leftpanel of Figure 1 with Equation (2), where the fitting results are shown with solid lines in this panel. One can find that the electron spectra in the letanel of Figure 1 can be well described with our empiricafunction. Then, our empirical function can be used to figure out the electron spectrum for the prompt emission, without specifying a certain physical model for the electron spectrum.

Bézier curve is a smooth curve defined by some given control points, which is wildly used in computer graphics and the related fields this paper, we adopt a simple four-ordetwo-dimensional Bézier curveyhich is created by four control points P_1 , P_2 , P_3 , and P_4 in two-dimensional space. In general, starts at P_1 going toward P_2 and arrives at P_2 coming from the direction of P_3 . Usually, it would not pass through Pand P3 unless these four points are in a line. However, these two points would determine the behavior of the Bézier curve between Pand P4.

It should be noted that the electron spectrum hich can be described with our empirical function, should be continuous. If not, such as will a Burgess et al. (2011), our empirical a good fit. In addition, freeing the electron spectrum in the first equivalent to having an empirical photon spectrum in the first place. First, the lowest power-law index of the photon spectrum our empirical electron spectrum in the synchrotron ehould be largerthan -2/3. Second,the the estimation for the electron spectrum could help us to better understand the energy dissipation process in a relativistic jet.

For a given electron spectrum, the observed synchrotron radiation flux at a given frequency v can be calculated as

$$f_n(n) = \frac{\sqrt{3}q_e^{3} G}{2p d_e^{2} m_e c^{2}} \grave{Q}_{g_{e,1}}^{*} F(n/n_e) n(g_e) dg_e,$$
 (3)

where $F(K) = X \hat{O}_{k}^{+1}$ $K_{5,3}(k)dk$, $K_{5/3}(k)$ is the modified Bessel function of 5/3 order, $n_c = 3q_e B^2 g_e^2 G(1 + Z)/C$ $(2p_e^m c)$ is the characteristic frequency of the electron with Lorentz factor in magnetic field B, Γ = 300 is the bulk Lorentz factor of the jet, dis the luminosity distance, and g and c are the electron charge, electron mass, and light speed, respectively.

Based on Equations(1) and (3), we can fit the radiation spectrum of the prompemission and obtain the corresponding electron spectrum. his is our proposed spectral-fitting method used to estimate the electron spectrum for the prompt emission in the electron spectrum for the prompt emission in the electron spectra based on the last 1% of iterations are also the synchrotron radiation scenario test our method, we perform a simple testing fitting on a synthetic data. The synthetic data are generated asfollows: (i) We create a synchrotron radiation spectrum based on a bump-shape electron spectrum. $Q_{0.01}^{2} = 4.01^{+0.01}_{-0.01}$, and p = $-3.83^{+0.15}_{-0.17}$ are similar to those of an example, the black dashed line in the middle panel of Figure 94, provided electron spectrum and example, the black dashed line in the middle panel of Figure 94, provided electron spectrum wever, the obtained values i.e., Equation (1) with $\log q_1 = 1$, $\log q_2 = 4$, $\log y_1 = 30$, of $\log y_1 = 26.99_{11.01}^{9.32}$ and $\log y_2 = 43.88_{1.99}^{2.33}$ deviate from i.e., Equation (1) with $\log g_{\rm e,1} = 1$, $\log g_{\rm m} = 4$, $\log y_{\rm 1} = 30$, $\log y_{\rm 2} = 43$, $\log y_{\rm 3} = 42$, $\log y_{\rm m} = 40$, and p = -3.7, is adopted as our electron spectrum. In addition, B = 30 Gs is taken. (ii) We alue of $\log Y_1$. It implies that the electron spectrum from our fold this synchrotron radiation spectrum through the instrumentapectralfittings are only robust in the low-energy and highresponse of the Fermi Gamma-ray BurstMonitor to create Poisson-distributedynthetic data, where the python source package threeML² (Vianello et al. 2015) is used. Then, we perform the spectral fitting based on the synthetic data. The spectral fitting is performed based on the Markov Chain Monte Carlo (MCMC) method to produce posterior predictions for the model parameters, e., $\log Y_1$, $\log Y_2$, $\log Y_3$, $\log g_m$, and p. The python source package emce(Foreman-Mackey et al. 2013) is used for our MCMC sampling, where N_{walkers} × N_{steps}= 10×10^5 is adopted and the initial 50% iterations are used for burn-in. The priors of gy_1 , $logy_2$, $logy_3$, $log g_m$, and p are set as uniform distribution in the range of (-30, 100), (10, 70), (30, 50), (3, 5), and (-5, -3), respectively The projections of

The radiation spectrum

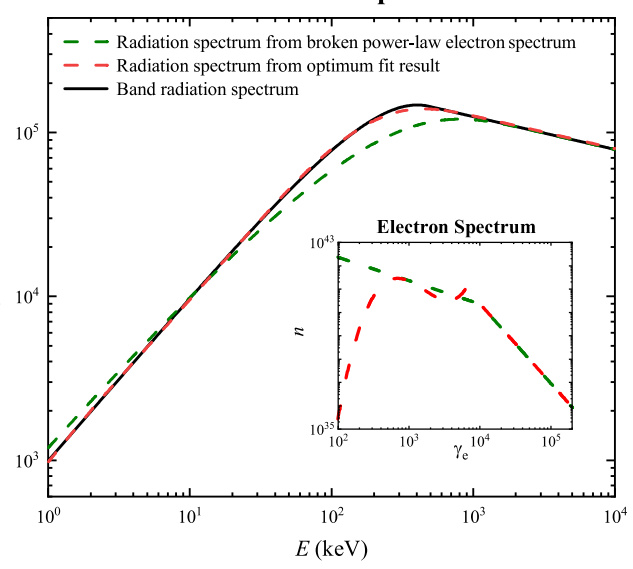


Figure 2. Band radiation spectrum (black line) and the related electron spectra (inset panel). Here a Band function with $\alpha = -1$, $\beta = -2.3$, and ± 400 keV is discussedThe inset plots the broken power-law electron spectrum and the electron spectrum obtained based on Equations (1) and (3). The corresponding synchrotron radiation spectra are shown with green and red dashed lines,

the posterior distribution in 1D and 2D for the model can find that the obtained values of $\log y_3 = 41.85^{+0.29}_{0.33}$ those of our provided electron spectrum especially for the energy ranges rather than the lowest-energy range.

3. Spectral Analysis

3.1. Comments on the Band Function

In this subsection, we investigate the electron spectrum related to the Band radiation spectrum in the synchrotron radiation scenario A Band function with typical parameters $\alpha = -1$, $\beta = -2.3$, and $E_p = 400$ keV is discussed in this subsection and shown in Figure 2 with a black line. In general, it is believed that such a radiation spectrum is originated from the synchrotron radiation of a broken powerlaw electron spectrum with p $_{low}$ = 2(α + 1) - 1 and p = 2 $(\beta + 1) - 1$, where p_{ow} and p are the low-energy and highenergy power-law indexes, respectively. The synchrotron https://github.com/dfm/emcee/blob/b9d6e3e7b1926009baa5bf422ae738d1 radiation spectrum of such an electron spectrum is shown in Figure 2 with a green dashed line. Obviously, the radiation spectrum generated from this kind of broken power-law electron spectrum is very different from a Band radiation spectrum, especially for the part around the transition from low-energy spectral segment to high-energy spectral segment. The transition is apparently sharp for the Band function compared with the synchrotron radiation spectrum. This behavior has also been found in many previous works, g.,

https://github.com/threeML/threeML

b06a848a/docs/index.rst

⁴ The priors of $\log Y_1$, $\log Y_2$, and $\log Y_3$ are set based on the following consideration. With Equation (2), we fit the electron spectra in the left panel of Figure 1. The fitting results reveathat the values of log y₃ and log y₂ do not deviate from the value of $\log V_4$ significantly. Therefore, we set the priors of $\log V_3$ and $\log V_2$ as $(\log V_4 - 10, \log V_4 + 10)$ and $(\log V_4 - 30, \log V_4 + 30)$, i.e., (30, 50) and (10, 70), respectively. In addition, the prilargov may be in a wide range. The reason can be found at the end of Section 2. Then, we set prior of $log Y_1$ as (-30, 100). Actually, we also try a wider range of the priors for these three parameters and obtain very similar fit results.

Zhang et al. (2016) and Burgess (2019)This result suggests that the Band radiation spectrum may nobe produced by a broken power-law electron spectrum.

In the following, we search for the most suitable electron spectrum for the Band radiation spectrum by fitting it with Equations (1) and (3). The obtained electron spectrum and its simulations are almost a bump or power-law shape in its lowradiation spectrum are shown in Figure 2 with a red dashed line. Although the obtained radiation spectrum is basically consistent with the Band radiation spectrunit, is a bit weird for the unexpected sharp peak at vand the strange bump at the low-energy regime of electron spectrum. We point out that this kind of electron spectrum may be unnatural to some degree. The reasons are shown as follows. (1) The peak at y is mainly related to the exponential-connected break in the Band function, whereas the physical origin of this break is not clear yet. (2) Although the obtained electron spectrum can produce a Band-like synchrotron radiation spectrum, the position of the low-energy bump and γ_m peak in electron spectrum should be fine-tuned, which may hardly exist in a real situation. (3) The shape of this electron spectrum is very different from those in the left panel of Figure 1, except the one shown with the green line, which has a similar peak at ~γ_m. However, one should note that this kind of electron spectrum mainly appears without making significant contribution to the observed flux (e.g., Uhm & Zhang 2014). Therefore, we would like to believe that the γ_m peak in the electron spectrum corresponding to the Band function may be an unnatural outcome. Then, the exponential transition in the Band function may not well describe the transition behavior in the radiation spectrum of the prompt emission if the synchrotron radiation does work.

This subsection is dedicated to studying the electron spectrum corresponding to the Band radiation spectrum in the analysis. The reason is presented athe end of this section. synchrotron radiation scenario. We found that the electron spectrum of the Band radiation spectrum may be hardly reproduced in a physical model, e.g., the models producing the electron spectrum in Figure 1. It suggeststhat the Band radiation spectrum may be not intrinsic to the prompt emission what was reported in Ravasio et al. (2019). Therefore,our of GRBs, especially to the transition segment between the low-energy regime and high-energy regiment the radiation spectrum. We would like to point out that to understand the characteristicsof the Band radiation spectrum, fitting the synthetic observed data of the synchrotron radiation with the Band function is necessary. For example, Burgess et al. (2015) simulate synchrotron orsynchrotron+blackbody spectra and fold them through the instrumental response of the Fermi Gamma-ray Burst Monitor. They then perform a standard data analysis by fitting the synthetic data with both Band and Band +blackbody models to investigate the ability of the Band function to fit a synchrotron spectrum within the observed energy band.

3.2. Application on GRBs 180720B and 160905A

In this subsection, we fit the radiation spectrum of GRBs 180720B and 160905A with Equations (1) to estimate the electron spectrum in the synchrotron radiation scenario. In our spectral analysis, we use the data from Fermi/GBM. GBM has 12 sodium iodide (NaI) scintillation detectorscovering the 8 keV-1 MeV energy band, and two bismuth germanate (BGO)scintillation detectors sensitive to the 200 keV-40 MeV energy band (Meegan at 2009). The brightest NaI and BGO detectors are used in our analyses. Thene spectral fitting based on narrow parameter areas.

python source package qtBurst⁵ is used to extract the light curves and source spectra. Xspec (Arnaud 1996; Atwood et al. 2009) is used to perform spectral analysis, where the "Poisson-Gauss" fitstatistic (i.e., pgstat) is adopted. The theoretical electron spectra from numerical calculations or energy regime (see the left panel of Figure 1). Then, Equation (1) is restricted to be a bump or power-law shape in our fittings. That is to say, the point (P_3) should be above or on the line of P_1P_4 (P_2P_4).

GRB 180720B Analysis. GRB 180720B is a long burst with a redshift z = 0.654 and detected by Fermand Swift satellites (Roberts & Meegan 2018; Bissaldi & Racusin 2018; Siegel et al. 2018; Vreeswijk et al. 2018). The obtained Nal 6 light curve of the promptemission is shown in the bottom insetf each panel in Figure 3, where the brightest NaI (i.e., NaI 6 and Nal 8) and BGO (i.e., BGO 0) detectors are used in our analyses. As an example, we first select a time period of [7.14, 8.19] s after the burst triggered for our analysis, which is marked with blue color in the bottom inset of the left panel in Figure 3. This time period is also used in the spectral analysis of Ravasio et al. (2019), of which the results can be used to compare with ours. The spectral fitting result is shown with a black line in the upper inset of the left panel. The corresponding electron spectrum is shown with a blue solid line in this panel and is also reported in Table 1. Inspired by the fit result in Section 2, this kind of electron spectrum can be decomposed into three segments lowest-energy segment (marked with pink shading)the low-energy segment (marked with yellow shading), and the high-energy segmen(marked with cyan shading). It should be noted that only the low-energy segment and the high-energy segment are robust in our One can find thatthe low-energy segment $\gamma_e \sim \gamma_m$ can be approximated $a\mathfrak{S}_e \mu \ g_e^2$, which is the low-energy electron espectrum in the standard fast-cooling pattern and is shown with a black dashed line in Figure 3This result is consistent with method is applicable to estimate the electron spectrum for the prompt emission in the synchrotron radiation scenario.

For the pulse in [7.14, 9.00] s, we also perform detail spectral analysis on the remaining time periods, e.g., [8.19, 8.70] s and [8.70, 9.00] s, which are marked with red and green colors in The inset of the middle panel of Figure 3, respectively. The obtained electron spectra forthese three time segmentare shown in the middle panel of Figure 3. The robust low-energy and high-energy segments n the electron spectraare also marked with yellow and cyan shading, respectively. From this panel, one can find that the morphology of the electron spectra varies with time in a pulse, especially the morphology of the low-energy segment. In terms of this pulse, the electron spectra

⁵ https://github.com/giacomov/gtburst

 $^{^6}$ The initial values of y_1 , y_2 , y_3 , and p are set as follows. First, the prompt emission is fitted with the Band function to obtain the optimum value of α , β , and E_0 . Then, B can be set by solving n_b ° 0.3′ $3q_eB^2g_{m_0}^2G(1+z)/(2pm_ec)=E_b$ ° $E_0(a-b)$, where E_b is the break photon energy of the Band function. In addition, the electron spectrum is initially set as a broken power law with $p_{low} = (\alpha + 1) \times 2 - 1$ and $p = (\beta + 1) \times 2 - 1$. y_m is set by equaling $f_v(v_b)/v_b$ to the photon flux of the Band function at E_b . In our fitting, y_1 , y_2 , y_3 , y_m , and p are the free parameters. Based on the above settings, we perform a tentative spectral fit to roughly estimate parameters in a relatively wide parametereas. With the obtained optimum fitting results from the tentative fitting, we further perform a

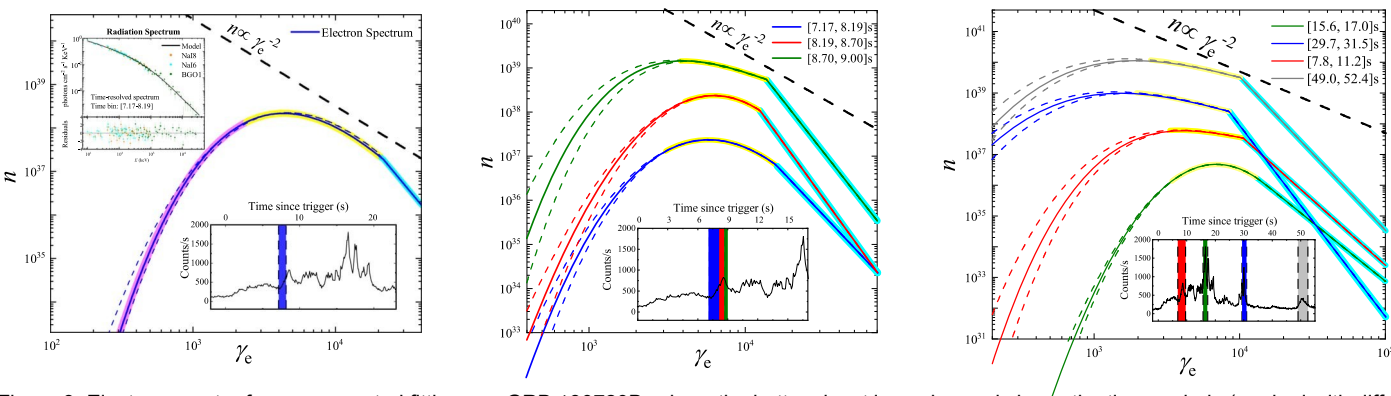


Figure 3. Electron spectra from our spectral fittings on GRB 180720B, where the bottom inset in each panel shows the time periods (marked with different colors) f spectral fittings and the corresponding electron spectrum is shown with solid lines and with the same color as that marked on the studied time period. The dashed below and above each solid lines are used to constrain the low-energy and high-energy segments in our obtain/ed electron typedtrition, the standard fastcooling electron spectrum g_e^2 is shown with a black dashed line in each panel. For convenience, the electron spectra of [8.19, 8.70] s, [8.70, 9.00] s, [7.8, 11.2] s [15.6, 17.0] s,[29.7, 31.5] s,and [49.0,52.4] s are shifted by timing 2030, 15, 0.1, 200, and 2000 factors respectively.

Table 1 Optimum Value of Parameters and the Corresponding pgstat/dino. Each Time Period

Burst	Time Period (s)	log y₁	log y ₂	log y ₃	log Y ₄ a	$\log g_{\rm m}$	р	B ^a	pgstat/d.o.f.
	[7.17 - 8.19]	0	36.94	40.86	37.28	4.34	-3.94	1473.89	343.12/341
	[8.19 - 8.70]	0	36.94	40.86	37.28	4.34	-3.94	2000.09	343.12/341
GRB	[8.70 - 9.00]	0	36.94	40.86	37.28	4.34	-3.94	1275.28	343.12/341
180720B	[7.8 - 11.2]	0	38.07	37.23	36.36	4.02	- 4.18	1863.36	428.06/341
	[15.6 - 17.0]	0	27.05	38.60	37.04	4.04	-3.75	1347.31	422.78/341
	[29.7 - 31.5]	22.77	38.39	37.24	36.10	3.93	-6.21	2603.91	409.18/348
	[49.0 - 52.4]	20.56	38.56	37.62	36.42	4.00	-4.99	1248.34	412.99/348
	[10.0 - 13.35]	-30	5.95	41.83	37.34	3.82	-3.64	3099.20	534.26/342
GRB	[13.35 - 14.65]	-20	10.21	40.23	36.65	3.77	-4.08	3001.39	342.40/341
160905A	[14.65 - 20.0]	-10	14.69	38.77	36.33	3.84	-3.70	1521.75	561.99/312
	[20.0 - 25.0]	23.24	39.29	37.69	36.10	3.90	-5.09	2521.53	400.12/307

Note.

in its low-energy regime can be very different from the standard fast-cooling pattern and even a broken power-law four pulses in this burst, which are in [7.8, 11.2] s (marked withfigure and also reported in Table 1. Same as Figure 3, the red color), [15.6, 17.0] s (marked with green color), [29.7, 31.5] s (marked with blue color), and [49.0, 52.4] s (marked of the right panel of Figure 3. The obtained electron spectra are very different from the standard fast-cooling patter The shown in the rightpanel of this figure with the same color as that marking on the studied time period. In terms of these pulses, the low-energy electron spectra can be also very different from the standard fast-cooling pattern and even a broken power-law functione.g., the pulse marked with green color.

GRB 160509A Analysis. It is clear that GRB 180720B consists of multiple emission episodes this paragraph, we would like to perform the spectral analysis for a burst with single contiguous and pulse-like structure, taking GRB 160509A as an exampleGRB 160509A is a long burst with redshift z = 1.17 and detected by Fermi and Swift

which are marked with green, red, blue, and gray colors, respectively. The obtained electron spectrum from spectral function. Besides, we also perform similar spectral analysis for fitting for each time period is shown with the same color in this robust low-energy and high-energy segments in the electron spectra are also marked with yellow and cyan shadow, with gray color), respectively. Please see the details in the insetespectively. One can find that the low-energy electron spectra

low-energy electron spectra in the time periods of [10–13.35] s, [13.35–14.65] s,and [14.65–20] s are presented as a narrow bump rather than a power-law function. The electron spectrum in the time period of [20–25] s is rather soft compared with other three electron spectral owever, its low-energy segment is presented as a power-law function with index ~-1.4 rather than -2.

At the end of this section, we present the reason why only the low-energy and high-energy segment in our obtained electron spectra are robust. This is owing to that the synchrotron emission of the electrons at the lowest-energy segmentmakes a negligible contribution to the total diation

satellites. The obtained NaI 0 light curve of the prompt spectrum. The synchrotron radiation spectrum of an individual emission is shown in the inset of Figure 4, where the brightest electron is $f_v \propto v^{1/3}$ for $v << v_c$. Thus, the electron spectrum Nal detector (Nal 0 and Nal 3) and BGO (BGO 0) detectors arewith a power-law index much larger than −1/3 would have a used for our analyses. Four different time periods are selected negligible effect on the radiation spectrum. Therefore, the [10–13.35] s, [13.35–14.65] s, [14.65–20] s, and [20–25] s, outline of the lowest-energy segment of the electron spectrum

^a The value of the quantities are fixed in the fitting.

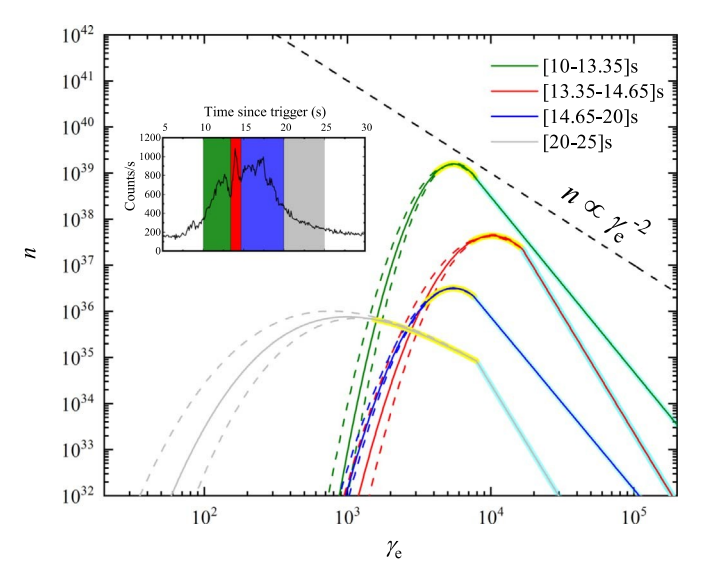


Figure 4. Electron spectra from our spectral fittings on GRB 160509A and the upper inset show the different time periods used for spectral analysis. For convenience, the electron spectra of [13.35-14.65] s, [14.65-20] s, and [20-25] s are also shifted by timing 0.01,00, and 1/15, respectively.

cannot be obtained by fitting the synchrotron radiation spectrum. To differentiate the lowest-energy segment from the robust low-energy segment, here we propose another simpler but more general method. Taking the spectral analysis (https://github.com/giacomov/gtburst), SciPy (Jones et al. in [7.19, 8.17] s of GRB 180720B as an example, we fix log y at two different values around its first best-fit value (for example, $\log y_1 = 5$ and -5 in here) and perform the twice independent fit again. The electron spectra obtained from twice fit are shown as two blue dashed lines around the electron spectrum of the first fit result. The overlap region of these threeDa-Bin Lin https://orcid.org/0000-0003-1474-293X spectra would be recognized as the robust low-energy segmenRui-Jing Lu® https://orcid.org/0000-0003-2467-3608 Conversely the divergence region would be recognized as the En-Wei Liang https://orcid.org/0000-0002-7044-733X lowest-energy segment.

4. Conclusions and Discussions

More and more evidence indicates that synchrotron radiation is a promising mechanism for the promptmission of GRBs. However, the electron spectrum for the prompt emission is diverse in numerical calculations or simulations. this paper. we propose a method to estimate the electron spectrum using Beniamini, P., Barniol Duran, R., & Giannios, D. 2018, MNRAS, 476, an empirical function, which is a four-order Bézier curve (lowenergy regime) jointed with a linear function (high-energy regime) in log-log coordinate. In the synchrotron radiation scenario with the electron spectrum described by our empirical Burgess, J. M., PreeceR. D., Baring, M. G., et al. 2011, ApJ, 741, 24 function, the following two works are studied in this paper. (1) The electron spectrum corresponding to the Band radiation spectrum is investigated. We find that the exponential transition baigne, F., Bošnjak, Ž, & Dubus, G. 2011, A&A, 526, A spectrum is investigated. We find that the exponential transition baigne, F., & Mochkovitch, R. 1998, MNRAS, 296, 275 of the Band radiation spectrum is more abrupt compared with that of the synchrotron radiation spectrum based on a broken power-law electron spectrum. Moreover, such exponential transition required a fine-tuned electron spectrumwhich is hardly produced in a real situation. Then, we suggest that it may be inappropriate to use the Band function to estimate the Ghisellini, G., Celotti, A., & Lazzati, D. 2000, MNRAS, 313, L1 electron spectrum for the prompemission of GRBs.(2) We perform the spectral analysis on the observations of the promp@uo,F.,Li, H., Daughton,W., & Liu, Y.-H. 2014,PhRvL,113, 155005 emission to estimate the electron spectrum. GRB 180720B and tools for Python,https://www.scipy.org/ GRB 160509A are studied as examples. By performing spectral aneko, Y., PreeceR. D., Briggs, M. S., et al. 2006, ApJS, 166, 298

that the morphology of the electron spectrum in its low-energy regime evolves with time in a burst and even in a pulse. In addition, it can be curved in some time periods, which is very different from the standard fast-cooling pattern (i.e. μ $g_{\rm p}^{2}$) and even a power-law function.

Our proposed method is used to estimate the electron spectrum for the prompt emission, without specifying a certain physical model for the electron spectrum. In this paper, we focus on the synchrotron radiation scenario Actually, one could imagine convolving this electron spectrum with other emission kernels may also getequally well-fitting solutions (pointed out by the referee). It would be very interesting to investigate the shape of the electron spectrum with other emission kernels.

We thank the anonymous referee of this work for useful comments and suggestions that proved the paper We also thank Qi Wang and Zhi-Lin Chen for the useful discussions and suggestionsThis work is supported by the National Natural Science Foundation of China (grant Nos. 11773007, 11533003, U1938106, U1731239), the Guangxi Science Founda tion (grant Nos. 2018GXNSFFA281010, 2017AD22006, 2018GXNSFGA281007, 2018GXNSFDA281033), and the Innovation Team and Outstanding Scholar Program in Guangxi Colleges. We acknowledge the use of public data from the Fermi Science Support Center (FSSC).

Software: Xspec (Arnaud 1996; Atwood et al. 2009), gtBurst 2001), emcee (Foreman-Mackeyet al. 2013), threeML (Vianello et al. 2015).

ORCID iDs

References

```
Arnaud, K. A. 1996, in ASP Conf. Ser., 101, Astronomical Data Analysis
                                                                               Software and Systems &d. G. H. Jacoby & J. Barnes (San Francisco, CA:
                                                                               ASP), 17
                                                                             Asano, K., & Terasawa, T. 2009, ApJ, 705, 1714
                                                                             Atwood, W. B., Abdo, A. A., Ackermann, M., et al. 2009, ApJ, 697, 1071
                                                                             Band, D., Matteson, J., Ford, L., et al. 1993, ApJ, 413, 281
                                                                             Baring, M. G., & Braby, M. L. 2004, ApJ, 613, 460
                                                                             Bissaldi, E., & Racusin, J. L. 2018, GCN, 22980,1
                                                                             Burgess, J. M. 2019, A&A, 629, A69
                                                                             Burgess, J. M., Bégué, D., Greiner, J., et al. 2020, NatAs, 4, 174
                                                                            Burgess, J. M., Preece R. D., Connaughton V., et al. 2014, ApJ, 784, 17
                                                                             Burgess, J. M., Ryde, F., & Yu, H.-F. 2015, MNRAS, 451, 1511
                                                                                                                           526, A110
                                                                            Derishev, E. V., Kocharovsky, V. V., & Kocharovsky, V. V. 2001, A&A,
                                                                               372, 1071
                                                                             Florou, I., Petropoulou M., & Mastichiadis, A. 2021, arXiv:2102.02501
                                                                             Foreman-MackeyD., Hogg, D. W., Lang, D., & Goodman, J. 2013, PASP,
                                                                             Ghirlanda, G., Celotti, A., & Ghisellini, G. 2002, A&A, 393, 409
                                                                             Goldstein, A., Burgess, J. M., Preece R. D., et al. 2012, ApJS, 199, 19
emission to estimate the electron spectrum. GRB 180720B and tools for Puther https://www.csi.n. 2001, SciPy: Open source scientific
analysis for a series of time periods in these two bursts, we find iang, E., Kusunose, M., Smith, I. A., & Crider, A. 1997, ApJL, 479, L35
```

```
Liu, K., Lin, D.-B., Wang, K., et al. 2020, ApJL, 893, L14
Lloyd, N. M., & Petrosian, V. 2000, ApJ, 543, 722
Lloyd-Ronning, N. M., & Petrosian, V. 2002, ApJ, 565, 182
Mao, J., & Wang, J. 2013, ApJ, 776, 17
Medvedev, M. V. 2000, ApJ, 540, 704
Meegan, C., Lichti, G., Bhat, P. N., et al. 2009, ApJ, 702, 791
Meszaros P., Rees, M. J., & Papathanassioud. 1994, ApJ, 432, 181
Nakar, E., Ando, S., & Sari, R. 2009, ApJ, 703, 675
Nava, L., Ghirlanda, G., Ghisellini, G., & Celotti, A. 2011, A&A, 530, A21
Oganesyan, G., Nava, L., Ghirlanda, G., Melandri, A., & Celotti, A. 2019,
A&A, 628, A59
```

Pe'er, A., & Zhang, B. 2006, ApJ, 653, 454 Preece R. D., Briggs, M. S., Mallozzi, R. S., et al. 1998, ApJL, 506, L23 Preece R. D., Briggs, M. S., Mallozzi, R. S., et al. 2000, ApJS, 126, 19 Ravasio, M. E., Ghirlanda, G., Nava, L., & Ghisellini, G. 2019, A&A, 625, A60
Roberts, O. J., & Meegan, C. 2018, GCN, 22981,1
Sari, R., Piran, T., & Narayan, R. 1998, ApJL, 497, L17
Siegel, M. H., Burrows, D. N., Deich, A., et al. 2018, GCN, 22973,1
Sironi, L., & Spitkovsky, A. 2009, ApJ, 698, 1523
Tavani, M. 1996, ApJ, 466, 768
Uhm, Z. L., & Zhang, B. 2014, NatPh, 10, 351
Vianello, G., Lauer, R. J., Younk, P., et al. 2015, arXiv:1507.08343
Vreeswijk, P. M., Kann, D. A., Heintz, K. E., et al. 2018, GCN, 22996, 1
Yang, Y.-P., & Zhang, B. 2018, ApJL, 864, L16
Zhang, B.-B., Uhm, Z. L., Connaughton, V., Briggs, M. S., & Zhang, B. 2016, ApJ, 816, 72
Zhao, X., Li, Z., Liu, X., et al. 2014, ApJ, 780, 12